

Evaluating scoring functions for docking and designing β -secretase inhibitors

M. Katharine Holloway,^{a,*} Georgia B. McGaughey,^a Craig A. Coburn,^b Shawn J. Stachel,^b Kristen G. Jones,^b Elizabeth L. Stanton,^b Alison R. Gregro,^b Ming-Tain Lai,^c Ming-Chih Crouthamel,^c Beth L. Pietrak^c and Sanjeev K. Munshi^d

^aDepartment of Molecular Systems, Merck Research Laboratories, PO Box 4, West Point, PA 19486, USA

^bDepartment of Medicinal Chemistry, Merck Research Laboratories, PO Box 4, West Point, PA 19486, USA

^cDepartment of Biological Chemistry, Merck Research Laboratories, PO Box 4, West Point, PA 19486, USA

^dDepartment of Structural Biology, Merck Research Laboratories, PO Box 4, West Point, PA 19486, USA

Received 13 September 2006; revised 19 October 2006; accepted 23 October 2006

Available online 25 October 2006

Abstract—Several simple scoring methods were examined for 2 series of β -secretase (BACE-1) inhibitors to identify a docking/scoring protocol which could be used to design BACE-1 inhibitors in a drug discovery program. Both the PLP1 score and MMFFs interaction energy (E_{inter}) performed as well or better than more computationally intensive methods for a set of substrate-based inhibitors, while the latter performed well for both sets of inhibitors.

© 2006 Elsevier Ltd. All rights reserved.

β -Secretase (also known as β -APP cleaving enzyme or BACE-1) is one of two proteases responsible for processing the membrane-bound amyloid precursor protein (APP) to the 40/42 residue β -amyloid peptide (A β), the primary constituent of the amyloid plaques observed in the brains of Alzheimer's patients.¹ Since BACE-1 cleavage of APP appears to be the rate-limiting step² in the production of A β and BACE-1 knockout mice show complete absence of A β with no significant side effects,³ BACE-1 appears to be an attractive therapeutic target in the treatment of Alzheimer's disease.

BACE-1 has been characterized as the first known example of a pepsin-like aspartyl protease that is membrane-tethered.⁴ A crystal structure of the soluble domain reveals a high degree of similarity to the tertiary structures of other mammalian and fungal aspartyl proteases.⁵ Given the availability of coordinates for BACE-1, as well as prior experience with renin⁶ and HIV-1 protease inhibitors,⁷ we were interested in identifying a rapid docking/scoring protocol that could aid in the design of BACE-1 inhibitors. A series of peptidom-

imetic inhibitors (**1–13**, Table 1) reported by Ghosh et al.⁸ served as an initial training set. Several scoring functions were evaluated and compared to a previous study using the more computationally intensive LIE⁹ and LIECE¹⁰ methods on the same set of inhibitors. As **1–13** are large substrate-based inhibitors spanning a wide range of activity (five orders of magnitude), a second training set of smaller hydroxyethylamine (HEA) inhibitors (**14–25**, Table 4) with a narrower activity range (2 orders of magnitude) was also examined to determine how sensitive the methods were to small structure/activity variations.

Models for inhibitors **1–11** were derived from the X-ray structures of **12**¹¹ and **13**¹² as bound in the BACE-1 active site. Models of inhibitors **14–25** were derived from the X-ray structure of a nonpeptide BACE-1 inhibitor.¹³ The flexibility of the R groups shown in Tables 1 and 4 was explored by generating 25–50 conformers using a distance geometry algorithm.¹⁴ The crystal structures of BACE-1 complexed with **12**¹¹ and with a nonpeptide BACE-1 inhibitor¹³ were employed for minimization of inhibitors **1–13** and **14–25**, respectively. The active site was defined by selecting all residues within 10 Å of any atom of the cognate ligand. All titratable enzyme residues were charged with the exception of one of the catalytic

Keywords: β -Secretase; BACE-1; Alzheimer's disease; MMFF; PMF; PLP; LIGSCORE; LUDI; X-score.

*Corresponding author. Tel.: +1 215 652 7425; fax: +1 215 652 4625; e-mail: kate_holloway@merck.com

Table 1. Substrate-based BACE-1 inhibitors designed by Ghosh et al.⁸

Compound	R ¹	R ²	R ³	K _i (nM)	ΔG (kcal/mol)
1	Boc-Asn	Me	Me	22423.0	−6.38
2	Boc-Asn	Me	CHMe ₂	3134.0	−7.55
3		Me	CHMe ₂	1129.0	−8.16
4	Boc-Val-Asn	Me	Me	61.4	−9.90
5	Boc-Val-Asn	Me	CHMe ₂	5.9	−11.30
6		Me	CHMe ₂	50.1	−10.02
7		Me	CHMe ₂	9.4	−11.02
8		Me	CHMe ₂	5808.0	−7.19
9		Me	CHMe ₂	2.5	−11.81
10		Me	CHMe ₂	8.0	−11.11
11		CH ₂ CHMe ₂	CHMe ₂	10491.0	−6.84
12	Glu-Val-Asn-Leu-Ψ-Ala-Ala-Glu-Phe			1.6	−12.06
13	Glu-Leu-Asp-Leu-Ψ-Ala-Val-Glu-Phe			0.3	−13.05

aspartic acids, Asp₂₂₈, which was protonated on the inner oxygen, OD1. All inhibitors were neutral. All poses were energy-minimized using the MMFFs force field¹⁵ in the rigid BACE-1 active site. The pose which resulted in the lowest conformational energy for the ligand was selected and the corresponding enzyme–ligand energy (E_{inter}) was compared to the observed $\text{p}K_i$ ($-\log K_i$) or pIC_{50} ($-\log \text{IC}_{50}$). Two distance-dependent ($\epsilon = 2r, 4r$) and a large constant ($\epsilon = 50$) dielectric were examined as a simple means to approximate solvation effects. The energy-minimized geometries which led to the best correlation with experimental activity (i.e., $\epsilon = 50$ for **1–13** and $\epsilon = 2r$ for **14–23**) were subsequently rescored using LUDI,¹⁶ PLP,¹⁷ PMF,¹⁸ LIGSCORE,¹⁹ and X-Score.²⁰

Models of inhibitors **1–11** and the energy minimized structures of **12–13** are shown overlaid in Figure 1. Only minor differences were observed between the X-ray and energy-minimized structures of **12** and **13**, with the exception of the P₃ and P₄ groups in **12** which have relatively high B factors in the crystal structure and do not make specific interactions with the enzyme.

A plot of the computed MMFFs E_{inter} versus observed $\text{p}K_i$ (see Fig. 2) reveals that compound **11** is an outlier. This behavior was previously observed using the LIE method.⁹ It is unclear whether this is due to the experimental observation or the computational approach, for example, solvation may play an important role, as suggested by a subsequent LIECE study¹⁰ which employed

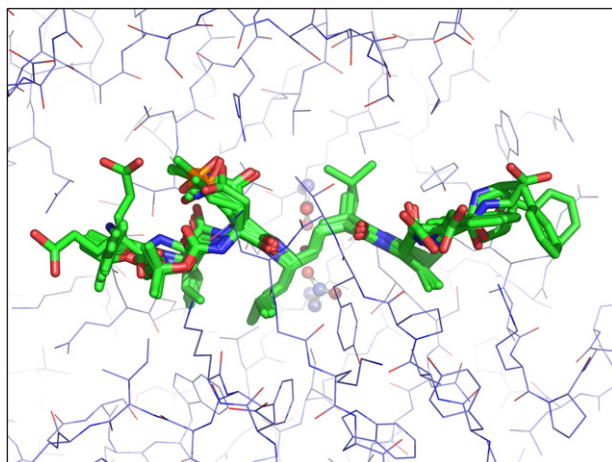


Figure 1. Overlay of the modeled structures for compounds **1–11** and the energy-minimized X-ray structures for **12** and **13** in the BACE-1 active site. The catalytic aspartates, Asp₃₂ and Asp₂₂₈, are shown in ball-and-stick mode. Image created using PyMol v0.98, DeLano Scientific LLC.

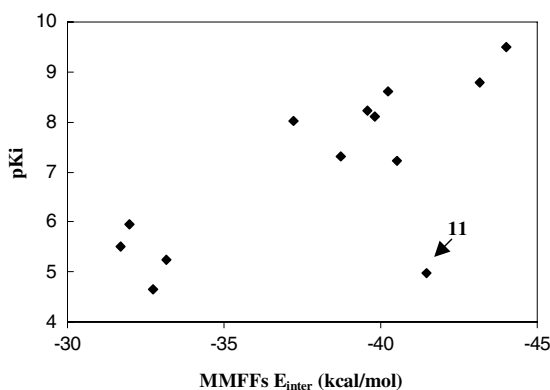


Figure 2. Plot of observed pK_i versus MMFFs E_{inter} ($\epsilon = 50$) for compounds **1–13**. Note that **11** is clearly an outlier.

a more accurate electrostatic solvation term. However, as this compound was an outlier with the LIE method and with all methods employed here, it has been excluded from further consideration in the correlations reported in Table 2.

Note that the scores from several methods correlated well with the observed pK_i values. The best were MMFFs energy ($\epsilon = 50$), LIGSCORE1, and PLP1/PLP2 with R^2 values of 0.85, 0.88, and 0.97/0.93, respectively.

Table 3 displays the predicted versus observed ΔG values for the MMFFs and PLP1 methods compared to the previous LIE⁹ and LIECE¹⁰ study and experimental results. The MMFFs E_{inter} alone leads to an rms difference of 0.79 kcal/mol, as compared to 1.10 and 0.92²¹ kcal/mol for LIE⁹ and LIECE.¹⁰ Subsequent rescoring of the MMFFs energy-minimized inhibitors using PLP1 leads to an improved rms of 0.34. It is apparent that, for this series of peptidomimetic inhibitors, energy minimization (\pm a scoring function) yields as good, if

Table 2. Correlation between computed score and inhibitor pK_i for inhibitors **1–13**

Scoring method	Ligand geometry	R^2
MMFFs, $\epsilon = 2r$	Minimized	0.73
MMFFs, $\epsilon = 4r$	Minimized	0.76
MMFFs, $\epsilon = 50$	Minimized	0.85
LIGSCORE1	MMFFs, $\epsilon = 50$	0.88
LIGSCORE2	MMFFs, $\epsilon = 50$	0.55
PLP1	MMFFs, $\epsilon = 50$	0.97
PLP2	MMFFs, $\epsilon = 50$	0.93
PMF	MMFFs, $\epsilon = 50$	0.62
LUDI	MMFFs, $\epsilon = 50$	0.03
X-Score	MMFFs, $\epsilon = 50$	0.31

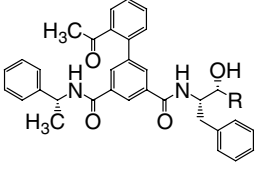
Table 3. A comparison of the free energy of binding (ΔG_{bind}) predicted for inhibitors **1–10**, **12–13** using the MMFFs E_{inter} ($\epsilon = 50$), the PLP1 score, and the LIE⁹ and LIECE^{10,21} methods

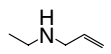
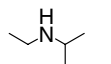
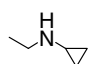
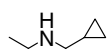
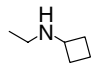
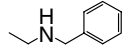
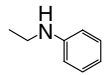
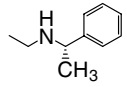
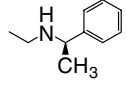
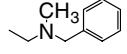
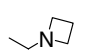
Compound	ΔG_{bind}				
	MMFFs	PLP1	LIE	LIECE	Exp.
1	−7.6698	−6.2047	−8.14	−6.47	−6.38
2	−7.1919	−7.4791	−8.92	−7.96	−7.55
3	−7.3160	−7.9636	−7.74	−7.67	−8.16
4	−11.2312	−10.0680	−11.17	−9.48	−9.90
5	−10.8084	−11.1181	−10.26	−11.53	−11.30
6	−10.4178	−10.4430	−10.38	−10.20	−10.02
7	−9.7331	−10.9074	−10.25	−11.12	−11.02
8	−7.8537	−7.7045	−8.31	−8.80	−7.19
9	−11.1163	−11.1349	−9.99	−10.21	−11.81
10	−10.9233	−11.5078	−9.94	−11.64	−11.11
12	−12.4489	−11.7321	−11.96	−10.05	−12.06
13	−12.8395	−13.2867	−12.98	−12.99	−13.05
rms	0.79	0.34	1.10	0.92	

The rms deviation for each method relative to the experimental^{8a} ΔG_{bind} is displayed below each column.

not better, agreement with experiment than the more computationally expensive LIE⁹ and LIECE¹⁰ methods. However, this set of inhibitors is large, substrate-based, and spans a wide range of activity. In order to assess how well the scoring protocol would perform on a typical drug-design problem, we employed a second test set of smaller, more drug-like HEA inhibitors **14–25**, shown in Table 4. This series of inhibitors, shown overlaid in Figure 3, varies solely in the substituent at the P1' position. The activity range²² is \sim 100-fold and includes **22** and **23** (*S* and *R* enantiomers, respectively) whose activity varies only 2-fold.

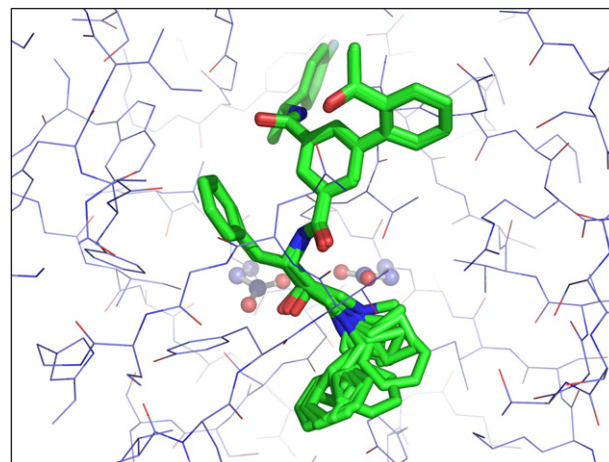
Table 5 shows the correlation between computed score and observed pIC_{50} for HEA inhibitors **14–23**. Inhibitors **24** and **25** were excluded from the correlations since they have indeterminate pIC_{50} values (i.e., $>10,000$ nM). In this instance, the MMFFs E_{inter} correlated best with experimental activity. There was little change in R^2 as the MMFFs dielectric constant was varied, possibly due to fewer H-bond interactions for **14–25** as compared to **1–13**. However, the best R^2 of 0.82 was achieved with a 2r distance-dependent dielectric. The MMFFs E_{inter} ($\epsilon = 2r$) scores for **14–25** are listed in Table 4. Note that the E_{inter} score was able to correctly rank the 2 enantiomeric inhibitors, **22** and **23**, with the former predicted,

Table 4. Peptidomimetic HEA inhibitors **14–25**, with variation at P1' and their corresponding MMFFs ($\epsilon = 2r$) E_{inter} values in kcal/mol


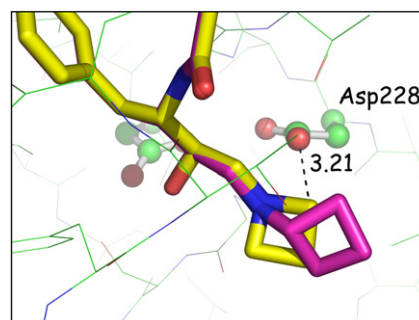
Compound	R	IC ₅₀ (nM)	E_{inter}
14	H	9900	−39.96
15		223	−46.38
16		674	−43.98
17		317	−45.42
18		418	−45.83
19		1400	−45.66
20		115	−50.07
21		110	−49.79
22		115	−50.36
23		348	−49.00
24		>10,000	−42.55
25		>10,000	−41.95

and observed, to be the more potent isomer. In addition, the calculated energy values for **24** and **25** are low (similar to R = H, **14**), in qualitative agreement with their poor activity. This can be rationalized by examining the inhibitors in the BACE-1 active site. As depicted in Figure 4, substitution of the HEA nitrogen causes a steric bump with the outside oxygen of one of the catalytic aspartates, Asp₂₂₈, which typically participates in an H-bond with the secondary amine.

In summary, we have demonstrated that simple scoring methods can perform as well or better than more computationally intensive methods for a series of substrate-based BACE-1 inhibitors. Additionally, one of the methods, MMFFs E_{inter} , also performed well for a series of HEA BACE-1 inhibitors. The MMFFs E_{inter} appears to be a simple, rapid scoring function which

**Figure 3.** Models of HEA inhibitors **14–25** bound in the BACE-1 active site.¹³ The catalytic aspartates, Asp₃₂ and Asp₂₂₈, are shown in ball-and-stick mode. Image created using PyMol v0.98, DeLano Scientific LLC.**Table 5.** Correlation between computed score and inhibitor pIC₅₀ for HEA inhibitors **14–23**

Scoring method	Ligand geometry	R^2
MMFFs, $\epsilon = 2r$	Minimized	0.82
MMFFs, $\epsilon = 4r$	Minimized	0.81
MMFFs, $\epsilon = 50$	Minimized	0.76
LIGSCORE1	MMFFs, $\epsilon = 2r$	0.26
LIGSCORE2	MMFFs, $\epsilon = 2r$	0.74
PLP1	MMFFs, $\epsilon = 2r$	0.69
PLP2	MMFFs, $\epsilon = 2r$	0.70
PMF	MMFFs, $\epsilon = 2r$	0.75
LUDI	MMFFs, $\epsilon = 2r$	0.49
X-Score	MMFFs, $\epsilon = 2r$	0.38

**Figure 4.** Models of HEA inhibitors **19** and **25** bound in the BACE-1 active site.¹³ Note the close contact between the azetidine ring and the outside oxygen of Asp₂₂₈. Image created using PyMol v0.98, DeLano Scientific LLC.

may be useful in a drug discovery program for rank-ordering virtual inhibitors in a high-throughput mode prior to synthesis.

References and notes

- Reviews include: (a) Vassar, R. *Adv. Drug Delivery Rev.* **2002**, 54, 1589; (b) Citron, M. *Neurobiol. Aging* **2002**, 23, 1017.

2. Sinha, S.; Lieberburg, I. *Proc. Natl. Acad. Sci. U.S.A.* **1999**, *96*, 11049.
3. Luo, Y.; Bolon, B.; Kahn, S.; Bennett, B. D.; Babu-Khan, S.; Denis, P.; Fan, W.; Kha, H.; Zhang, J.; Gong, Y.; Martin, L.; Louis, J.-C.; Yan, Q.; Richards, W. G.; Citron, M.; Vassar, R. *Nat. Neurosci.* **2001**, *4*, 231.
4. Vassar, R.; Bennett, B. D.; Babu-Khan, S.; Kahn, S.; Mendiaz, E. A.; Denis, P.; Teplow, D. B.; Ross, S.; Amarante, P.; Loeloff, R.; Luo, Y.; Fisher, S.; Fuller, J.; Edenson, S.; Lile, J.; Jarosinski, M. A.; Biere, A. L.; Curran, E.; Burgess, T.; Louis, J.-C.; Collins, F.; Treanor, J.; Rogers, G.; Citron, M. *Science* **1999**, *286*, 735.
5. Hong, L.; Koelsch, G.; Lin, X.; Wu, S.; Terzyan, S.; Ghosh, A. K.; Zhang, X. C.; Tang, J. *Science* **2000**, *290*, 150.
6. Williams, P. D.; Perlow, D. S.; Payne, L. S.; Holloway, M. K.; Siegl, P. K. S.; Schorn, T. W.; Lynch, R. J.; Doyle, J. J.; Strouse, J. S.; Vlasuk, G. P.; Hoogsteen, K.; Springer, J. P.; Bush, B. L.; Halgren, T. A.; Richards, A. D.; Kay, J.; Veber, D. F. *J. Med. Chem.* **1991**, *34*, 887.
7. Holloway, M. K.; Wai, J. M.; Halgren, T. A.; Fitzgerald, P. M. D.; Vacca, J. P.; Dorsey, B. D.; Levin, R. B.; Thompson, W. J.; Chen, L. J.; deSolms, S. J.; Gaffin, N.; Ghosh, A. K.; Giuliani, E. A.; Graham, S. L.; Guare, J. P.; Hungate, R. W.; Lyle, T. A.; Sanders, W. M.; Tucker, T. J.; Wiggins, M.; Wiscount, C. M.; Woltersdorf, O. W.; Young, S. D.; Darke, P. L.; Zugay, J. A. *J. Med. Chem.* **1995**, *38*, 305.
8. (a) Ghosh, A. K.; Bolcer, G.; Harwood, C.; Kawahama, R.; Shin, D.; Hussain, K. A.; Hong, L.; Loy, J. A.; Nguyen, C.; Koelsch, G.; Ermolieff, J.; Tang, J. *J. Med. Chem.* **2001**, *44*, 2865; (b) Ghosh, A. K.; Shin, D.; Downs, D.; Koelsch, G.; Lin, X.; Ermolieff, J.; Tang, J. *J. Am. Chem. Soc.* **2000**, *122*, 3522.
9. Tounge, B. A.; Reynolds, C. H. *J. Med. Chem.* **2003**, *46*, 2074; Rajamani, R.; Reynolds, C. H. *Bioorg. Med. Chem. Lett.* **2004**, *14*, 4843.
10. Huang, D.; Cafisch, A. *J. Med. Chem.* **2004**, *47*, 5791.
11. Hong, L.; Koelsch, G.; Lin, X.; Wu, S.; Terzyan, S.; Ghosh, A. K.; Zhang, X. C.; Tang, J. *Science* **2000**, *290*, 150.
12. Hong, L.; Turner, R. T., III; Koelsch, G.; Shin, D.; Ghosh, A. K.; Tang, J. *J. Biochem.* **2002**, *41*, 10963.
13. Coburn, C. A.; Stachel, S. J.; Li, Y.-M.; Rush, D. M.; Steele, T. G.; Chen-Dodson, E.; Holloway, M. K.; Xu, M.; Huang, Q.; Lai, M.-T.; DiMuzio, J.; Crouthamel, M.-C.; Shi, X.-P.; Sardana, V.; Chen, Z.; Munshi, S.; Kuo, L.; Makara, G. M.; Annis, D. A.; Tadikonda, P. K.; Nash, H. M.; Vacca, J. P. *J. Med. Chem.* **2004**, *47*.
14. In-house distance geometry program written using the theory and algorithms from: *Research Studies Press*; Crippen, C. M., Havel, T. F., Bawden, D., Eds.; Wiley: New York, 1988, and; Kuszewski, J.; Nilges, M.; Brunger, A. T. *J. Biomol. NMR* **1992**, *2*, 33.
15. (a) Halgren, T. A. *J. Comput. Chem.* **1996**, *17*, 490, 520, 553, and 616; (b) Halgren, T. A.; Nachbar, R. B. *J. Comput. Chem.* **1996**, *17*, 587.
16. Bohm, H. J. *J. Comput.-Aided Mol. Design* **1994**, *8*, 243.
17. (a) Gehlhaar, D. K.; Verkhivker, G. M.; Rejto, P. A.; Sherman, C. J.; Fogel, D. B.; Fogel, L. J.; Freer, S. T. *Chem. Biol.* **1995**, *2*, 317; (b) Verkhivker, G. M.; Bouzida, D.; Gehlhaar, D. K.; Rejto, P. A.; Arthurs, S.; Colson, A. B.; Freer, S. T.; Larson, V.; Luty, B. A.; Marrone, T.; Rose, P. W. *J. Comput. Aided Mol. Des.* **2000**, *14*, 731.
18. Muegge, I.; Martin, Y. C. *J. Med. Chem.* **1999**, *42*, 791.
19. Cerius2, version 4.6, revision 01.0901; Accelrys Inc. <http://www.accelrys.com/>.
20. Wang, R.; Lu, Y.; Fang, X.; Wang, S. *J. Chem. Inf. Comput. Sci.* **2004**, *44*, 2114.
21. The predicted pK_i was computed from Tables 1 and 2 of reference 10. Compound 11 was omitted from the rms calculation.
22. IC₅₀'s were determined as described in: Pietrak, B. L.; Crouthamel, M.-C.; Tugusheva, K.; Lineberger, J. E.; Xu, M.; DiMuzio, J. M.; Steele, T.; Espeseth, A. S.; Stachel, S. J.; Coburn, C. A.; Graham, S. L.; Vacca, J. P.; Shi, X.-P.; Simon, A. J.; Hazuda, D. J.; Lai, M.-T. *Anal. Biochem.* **2005**, *342*, 144.